Harmonic analysis of the stability of reverse routing in channels

M. Bruen, J. C. I. Dooge

Hydrol. Earth Syst. Sci., 11(1), 559–568, 2007
www.hydrol-earth-syst-sci.net/11/559/2007

Hydrology & Earth System Sciences

Harmonic analysis of the stability of reverse routing in channels

M. Bruen and J.C.I. Dooge

Centre for Water Resources Research, University College Dublin, Earlsfort Terrace, Dublin 2, Ireland

Email for corresponding author: michael.bruen@ucd.ie

Abstract

Normal downstream routing of a flood flow is a highly stable process for Froude numbers less than 1 and hence the results are reliable. In contrast, reverse routing in an upstream direction, which may be required for flow control, is potentially unstable. This paper reports the results of a study of the practical limits on channel lengths for reverse routing. Harmonic analysis is applied to the full non-linear solution of the St. Venant equations for three different wave patterns and two different wave periods, for a particular channel with a Froude number of 0.5. Reverse routing can be done for prismatic channels longer than 100 km. For long periods (>10 hours) the shape of the upstream hydrograph is recovered well. However, when the wave period is short (< 1hour), the high frequency components of the upstream hydrograph and, thus, its shape, are not recovered. These limits are influenced by the channel morphology and shape of the wave. Further work is needed to determine how these factors interact.

Keywords: floods, open channel flow, reverse routing, stability, harmonic analysis

Practical use of reverse routing

The topic of downstream direct routing of an upstream input to a free surface channel is well established in both hydrological theory and practice. Closed form solutions can be derived for linearised versions of the basic equations (Napiorkowski, 1992) and efficient methods have been developed for numerical solutions of the more general non-linear equations. The inverse problem of reverse routing from the downstream outflow back to the upstream inflow has not been studied to the same extent.

The reverse routing problem is a subject of both practical and theoretical interest. One of the earliest applications was in 'gate-stroking', i.e. the downstream control of the supply of water at various points in irrigation canals (as reviewed by Bodley and Wylie, 1978; Bautista *et al.*, 1997; Clemmens, 1998). The corresponding problem of determining the optimum control of an upstream reservoir to reduce downstream flooding at critical sites has been studied to a lesser extent. Reliable techniques would be of practical value in dealing with the problem of urban flooding due to flash floods, which is becoming a matter of increasing concern and attention.

Szollosi-Nagy(1987) applied the conceptual model of a linear discrete cascade as the basis of a reverse routing procedure to the severe, August 1980, flood of the Fekete-Kores River in Hungary. Nachlik and Witt (1990, 1993) used numerical computation to study the problem of reservoir control on the Dunajec River, a tributary of the upper Vistula, in Poland.

The work reported in this paper extends research in the 1990s, supported by the EU project TELFLOOD (Forecasting Floods in Urban Areas downstream of steep catchments). In that project, the reverse routing work was a prognostic approach to defining the limits to stability in reverse routing (Bruen and Dooge, 1999; Dooge and Bruen, 2005)

Basic equations of open channel flow

The basic formulation of unsteady one-dimensional flow in open channels is due to St. Venant (1871). He wrote the continuity equation as

$$\frac{\partial Q}{\partial x} + \frac{\partial A}{\partial t} = 0 \qquad (1)$$

where $Q(x,t)$ is the discharge and $A(x,t)$ the area of flow. He

wrote the momentum equation in terms of elevation, z, and velocity, u, i.e.

$$\frac{\partial z}{\partial x} + \frac{1}{g}\frac{\partial u}{\partial t} + \frac{u}{g}\frac{\partial u}{\partial x} + \frac{\tau_0 P}{\gamma A} = 0 \qquad (2)$$

where $z(x,t)$ is the elevation of the water surface, $u(x,t)$ is the velocity of flow, $A(x,t)$ is the cross-sectional area of flow and $P(x,t)$ its wetted perimeter, $\tau_0(x,t)$ is the boundary shear, g is the acceleration due to gravity, and γ is the weight density of water. For a prismatic channel, the momentum equation can be written in terms of discharge, Q, and cross-sectional area A, i.e. in the 2-dimensional state space form, as

$$\frac{1}{B}\frac{\partial A}{\partial x} + \frac{1}{gA}\frac{\partial}{\partial x}\left(\frac{Q^2}{A}\right) + \frac{1}{gA}\frac{\partial Q}{\partial t} = S_0 - \frac{n^2}{A^2 R^{4/3}}|Q|Q \qquad (3)$$

where, $B = \frac{\partial A}{\partial z}$ is the top-width of the water surface and z is its elevation.

Equations (1), (2) and (3) or their equivalents are the basic equations for both direct routing and reverse routing. For a solution, two boundary conditions and two initial conditions are required for the problem to be well-posed. However, (because of the non-linear form of the momentum equation), no analytical solution of the full St. Venant equations has been found and either analytical solutions of simplified versions of the equations, or numerical solutions to the discretised equations are sought.

Numerical solutions by finite differences

The non-linear open channel flow equations can be discretised in a four-point Preissman scheme (Preissman, 1961) similar to that used by Szymkiewicz (1993, 1996), Fig. 1.

The scheme is defined by prescribing how space and time derivatives of any quantity, say F, are to be approximated, Eqns. (4) and (5);

$$\frac{\partial F}{\partial t} = \Psi\frac{F_i^{j+1} - F_i^j}{\Delta t} + (1-\Psi)\frac{F_{i+1}^{j+1} - F_{i+1}^j}{\Delta t} \qquad (4)$$

$$\frac{\partial F}{\partial x} = (1-\theta)\frac{F_{i+1}^j - F_i^j}{\Delta x} + \theta\frac{F_{i+1}^{j+1} - F_i^{j+1}}{\Delta x} \qquad (5)$$

and how the value of F at the point P is be approximated, Eqn. (6);

$$F_p = \Psi\left[\theta F_i^{j+1} + (1-\theta)F_i^j\right] + (1-\Psi)\left[\theta F_{i+1}^{j+1} + (1-\theta)F_{i+1}^j\right] \qquad (6)$$

This discretisation scheme can be applied to the continuity and momentum equations to yield a set of finite difference equations which, given appropriate initial and boundary conditions, can be solved simultaneously for the unknown variables at each time step (forward routing) or, given a downstream hydrograph and appropriate initial and final time conditions, can be solved for the unknown variables at a previous space step (reverse routing) (Dooge and Bruen, 2005).

Fourier analysis

Fourier analysis is a well established method of examining time-series, Chatfield (1975). It determines the contribution to an individual time series of individual sinusoidal components of different frequencies. It considers that a time series can be represented as a sum of such sinusoidal components, Eqn. (7),

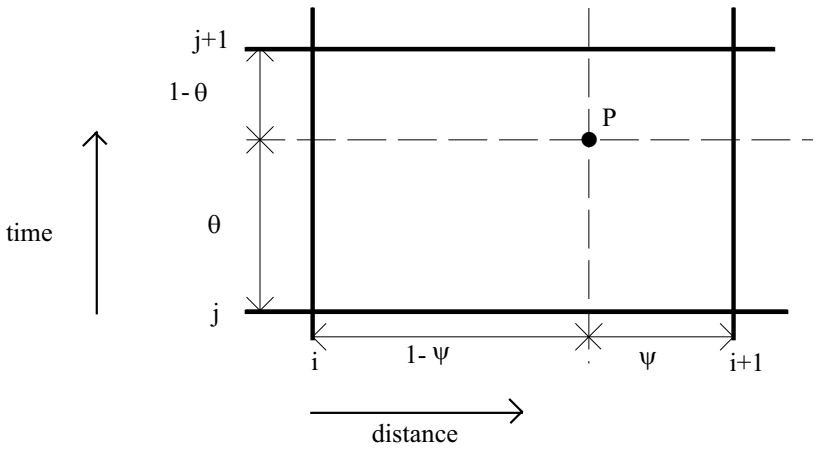

Fig. 1. *Four-point discretisation scheme*

$$x(k) = a_0 + \sum_{j=1}^{n/2-1}\left[a_j \cos(2\pi jk/n) + b_j \sin(2\pi jk/n)\right] + a_{n/2}\cos(\pi k) \quad (7)$$

The coefficients a_j and b_j can be estimated as follows:

$$a_j = \frac{2}{n}\left[\sum x_k \cos(2\pi jk/n)\right] \quad (8)$$

and

$$b_j = \frac{2}{n}\left[\sum x_k \sin(2\pi jk/n)\right] \quad (9)$$

The periodogram (Chatfield, 1975) is proportional to r_j^2, where

$$r_j^2 = a_j^2 + b_j^2 \quad (10)$$

and is used as a quantitative indication of the contribution of a particular frequency to the time series.

Input series used

Three different input series were tested for this paper. (i) a single wave of sinusoidal shape, starting from a base flow of 500 $m^3 s^{-1}$, rising to a peak of 4500 $m^3 s^{-1}$ and falling back to the 500 $m^3 s^{-1}$ base. The period of the sinusoidal shape is 1 hour. (ii) a train of ten such sinusoidal waves and (iii) a step function, stepping from 500 $m^3 s^{-1}$ up to 4500 $m^3 s^{-1}$and dropping back after 1 hour. This is physically unrealistic, but is instructive to see the effects of the discontinuities on the reverse routing. The input shapes are shown in Fig. 2 and the corresponding periodograms are in Fig. 3.

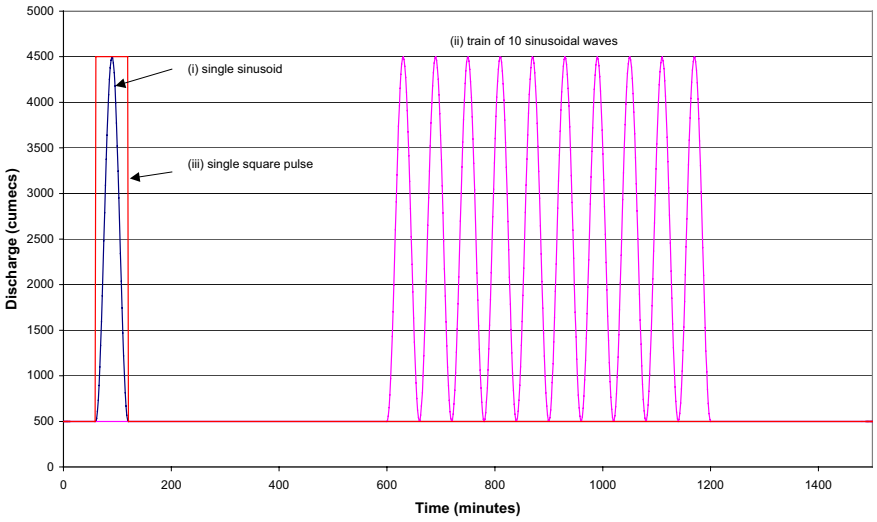

Fig. 2. *Inflow hydrographs used*

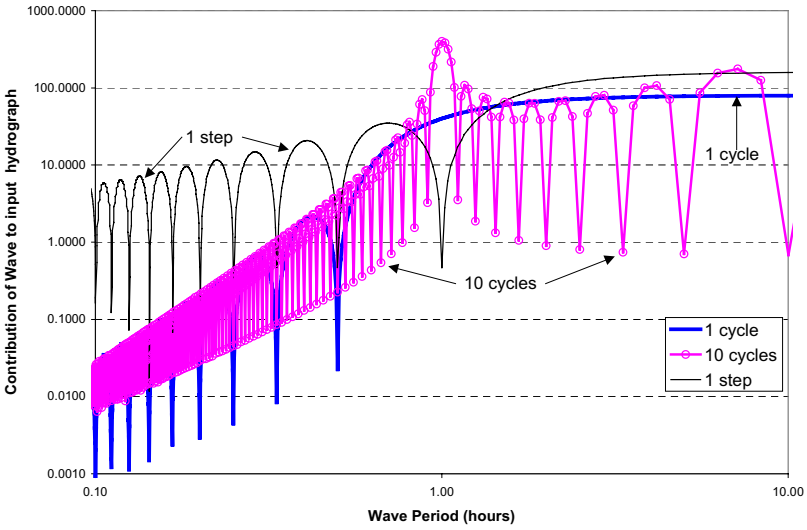

Fig 3. *Fourier analysis of input hydrographs from waves of period 6 minutes to 10 hours*

Methodology

In this study, the stability of reverse routing has been investigated using a Fourier Analysis. Upstream inflow floods are generated and routed through a long prismatic channel to give a downstream outflow hydrograph. Then, using only this hydrograph and the knowledge that the initial conditions were a steady base flow throughout the river, the outflow hydrograph is reverse routed in an attempt to recover the original upstream inflow. The periodogram of all the time-series involved is calculated and the attenuation of particular frequencies in the downstream routing and their magnification in reverse routing is estimated.

The numerical calculations were made for a 100 km reach of a 100 m wide rectangular channel using Manning's friction law with $n = 0.025$. The upstream boundary condition was a specified flow hydrograph. Three patterns of flood waves were used, but all rose from a base flow of 500 $m^3 s^{-1}$ to a maximum of 4500 $m^3 s^{-1}$ and fell back to the 500 $m^3 s^{-1}$ base. The first shape was a single sinusoid of a specified period, the second a train of ten such sinusoids and the third was a single step of specified duration. This last involves an instantaneous rise and subsequent fall in discharge and is unrealistic in practice but represents a very extreme case. It is included in the test because it contains high frequency Fourier components. Two different periods (or duration of the step) were used, 1 hour and 10 hours. The former represents an extreme case of a short duration flash flood and the latter period is more usual. A longitudinal channel slope of 0.000971 was used, which gives a Froude number of 0.5 at the mean flow of 2500 $m^3 s^{-1}$, mid-way between the base flow and the peak. The tests were performed with a channel length of 100 km as previous work had shown that reverse routing over this distance was possible (Dooge and Bruen, 1995). The downstream boundary condition was a uniform flow condition. To avoid possible complications with this condition, it was imposed 200 km downstream of the inflow. In effect, a 200 km reach of channel was simulated and the outflow was taken from the middle as the outflow from a 100 km reach of channel.

Results

INFLOW HYDROGRAPHS

The three inflow shapes used (single sinusoid, train of 10 sinusoids and step of 1hour period) are shown in Fig. 2. The contribution to each of these shapes from sinusoids of different wave periods (Fig. 3) are plotted in terms of period (rather than frequency) as it is easier to relate to waves in channels. The train of sinusoids has a local peak contribution at a period of 1hour, as might be expected; however, it has side-lobes over the entire spectrum, due to the finite duration of the train and the constant pre- and post-train flows. The single cycle has a more uniform contribution from the longer periods and fewer side-lobes. The square pulse has substantially more contribution from the shorter periods (higher frequencies) as might be expected from its unrealistically sharp transitions.

DOWNSTREAM HYDROGRAPHS

The downstream hydrographs produced by the numerical routing, using the full non-linear equations, are shown in Fig. 4 for the 1hour period inflow shapes. Note that, of the single wave shapes, the peak of the square pulse is

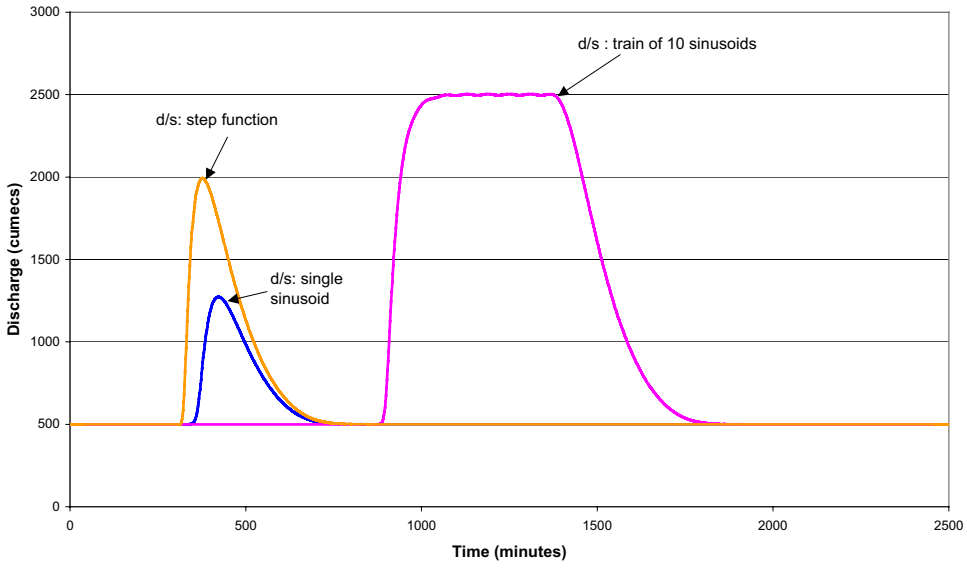

Fig. 4. *Downstream hydrographs (100 km downstream of inflow)*

considerably higher than that of the single sinusoid, although both inputs had the same peak, and its flat peak has been rounded. The individual waves of the 10-wave train have been effectively combined and the outflow is now essentially a single, flat-topped, wave. The information about the individual components of the train has been lost. A Fourier analysis of these wave shapes shows that the high frequency components of the inflow hydrograph have been strongly attenuated (Fig. 5). Dividing the periodogram of the downstream hydrographs by that of the upstream inflows gives a measure of the attenuation in the forward routing (Fig. 6). The curves are complex because they contain spurious short spikes at frequencies which are not well represented in the inflow, but all three show a strong drop in the contribution in the downstream hydrograph as the wave period drops from 10 hours to 1 hour.

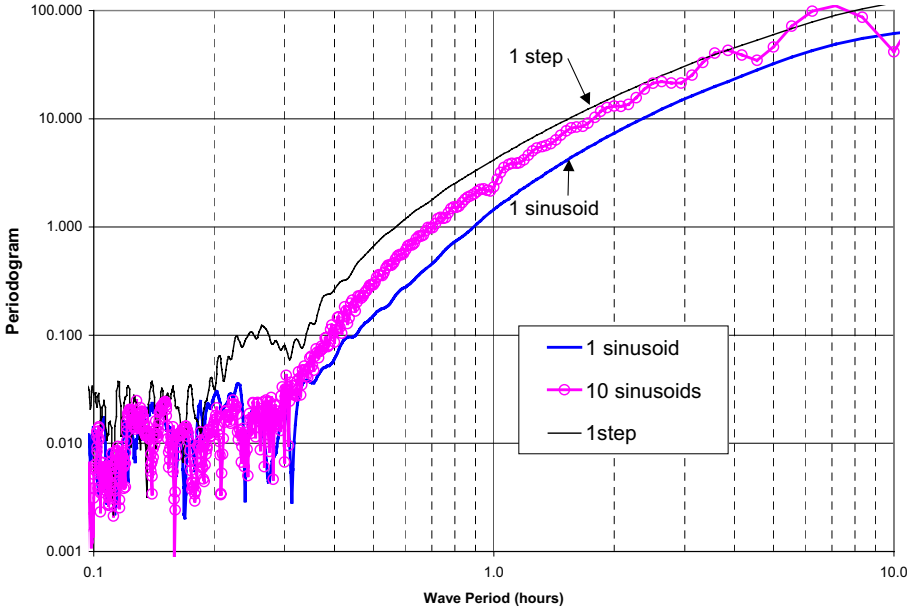

Fig. 5. *Fourier analysis of downstream hydrographs*

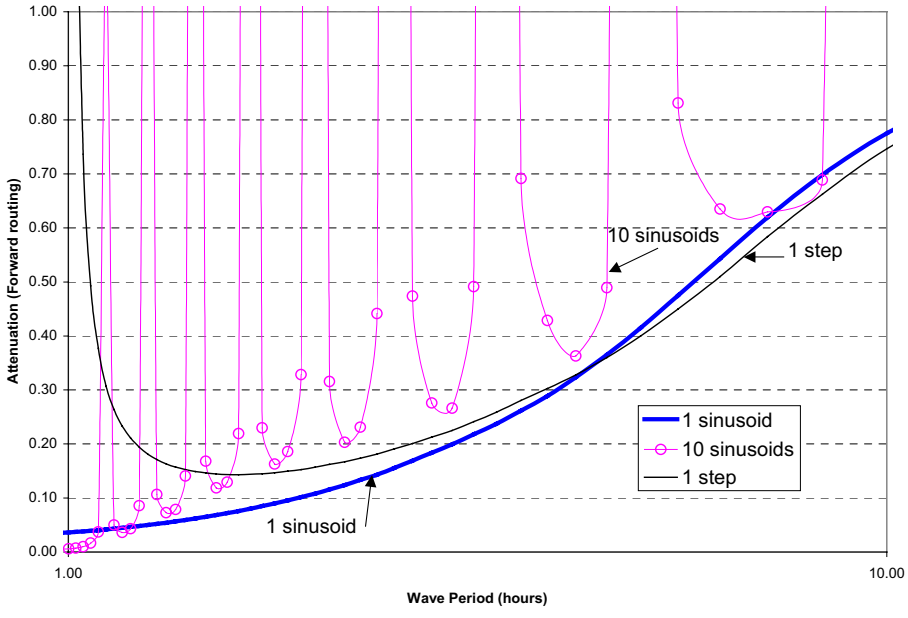

Fig. 6. *Attenuation of waves in forward routing*

Reverse routing

In linear situations, reverse routing would magnify the higher frequencies and the inverse of Fig. 6 would apply. However, the linear analysis does not apply to the full non-linear equations, so the reverse routing is investigated by numerical experimentation. The main parameters which can be adjusted for reverse routing are ϑ and Ψ, which specify the discretisation point within the four-point grid in time and space respectively. Tables 1 to 3 show the results of attempting to reverse route the three outflows of Fig. 4 back up the 100 km channel. The bold entries indicate where the routing was a success and the number is the peak discharge of the resulting upstream hydrograph (the actual inflow hydrographs all had peaks of 4500 cumecs). The rest of the entries indicate that the routing was not successful and the

Table 1. Results of Nonlinear Reverse Routing of the single sinusoid wave of period 1 hour

	0.9	1	1	3	4	6	10	28	74	100
	0.8	1	2	3	5	8	15	52	84	**1480**
	0.7	1	3	4	6	12	33	72	97	**1458**
	0.6	2	4	6	9	21	44	80	**1496**	**1439**
ϑ	0.5	4	5	8	16	31	61	90	**1469**	**1418**
	0.4	3	5	8	15	39	73	100	**1451**	**1399**
	0.3	2	5	7	12	30	85	**1484**	**1427**	**1381**
	0.2	1	4	6	10	21	95	**1461**	**1408**	**1360**
	0.1	1	3	5	8	15	**1500**	**1440**	**1390**	**1342**
		0.1	0.2	0.3	0.4	0.5	0.6	0.7	0.8	0.9
						Ψ				

Table 2. Results of Nonlinear Reverse Routing of the 10 sinusoids wave of period 1 hour

	0.9	1	1	1	4	6	9	19	85	**2612**
	0.8	1	1	3	5	8	14	51	99	**2583**
	0.7	1	3	5	8	12	28	68	**2613**	**2561**
	0.6	3	5	7	11	23	43	94	**2584**	**2545**
ϑ	0.5	4	6	9	17	29	52	**2614**	**2562**	**2533**
	0.4	4	6	9	17	36	67	**2585**	**2546**	**2524**
	0.3	1	5	8	13	32	83	**2563**	**2534**	**2518**
	0.2	1	4	7	10	20	98	**2547**	**2525**	**2513**
	0.1	1	1	5	8	14	38	**2535**	**2518**	**2509**
		0.1	0.2	0.3	0.4	0.5	0.6	0.7	0.8	0.9
						Ψ				

Table 3. Results of Nonlinear Reverse Routing of the single step wave of duration 1 hour

	0.9	1	1	2	4	5	9	18	61	89
	0.8	1	1	3	4	7	13	45	78	96
	0.7	1	3	4	6	10	25	69	90	98
	0.6	2	4	5	9	19	40	79	95	100
ϑ	0.5	3	5	8	16	29	52	88	97	**2487**
	0.4	3	5	8	15	35	73	94	99	**2435**
	0.3	2	5	7	11	26	82	97	**2486**	**2389**
	0.2	1	4	6	9	17	92	99	**2436**	**2342**
	0.1	1	1	5	7	12	38	100	**2390**	**2299**
		0.1	0.2	0.3	0.4	0.5	0.6	0.7	0.8	0.9
						Ψ				

number indicates the distance in km, measured from the downstream end, of the location of failure. Thus, for the single sinusoidal wave and $\Phi = 0.5$ and Ψ=0.5, the routing failed at 31 km from the downstream end. Failure is deemed to occur if the values of depth or discharge become negative. The calculated wave shape may become quite unrealistic and unusable even before this type of failure occurs. Although there are differences between the different inputs, all show success for lower values of Φ and higher values of Ψ. In all cases, the reverse routed hydrograph has a smaller peak discharge than the original inflow.

Tables 4 to 6 show the corresponding results for inflow wave periods of 10 hours. Figure 7 superimposes the reverse routing result on the original inflow hydrograph for the case of the single sinusoid with a 10-hour period. There is a good match of timing and only a slight reduction in recovered

Table 4. Results of Non-linear Reverse Routing of the single sinusoid wave of period 10 hours

	0.9	1	1	1	2	5	8	13	30	**4377**
	0.8	1	1	2	4	7	12	28	**4385**	**4370**
	0.7	1	2	4	6	10	22	73	**4378**	**4363**
	0.6	2	4	6	10	21	45	**4387**	**4372**	**4356**
ϑ	0.5	4	6	9	17	30	56	**4380**	**4365**	**4350**
	0.4	4	6	9	17	39	73	**4373**	**4358**	**4343**
	0.3	1	5	8	12	28	95	**4367**	**4351**	**4336**
	0.2	1	2	6	9	16	46	**4360**	**4344**	**4329**
	0.1	1	1	4	7	11	22	**4353**	**4338**	**4322**
		0.1	0.2	0.3	0.4	0.5	0.6	0.7	0.8	0.9
						Ψ				

Table 5. Results of Non-linear Reverse Routing of the 10 sinusoids wave of period 10 hours

	0.9	1	1	1	2	5	7	13	29	**4379**
	0.8	1	1	2	4	6	11	28	97	**4370**
	0.7	1	2	4	6	10	22	71	**4379**	**4363**
	0.6	2	4	6	10	20	42	94	**4372**	**4356**
ϑ	0.5	4	6	9	18	29	54	**4380**	**4365**	**4350**
	0.4	4	6	9	17	37	69	**4373**	**4358**	**4343**
	0.3	1	5	8	12	27	94	**4367**	**4351**	**4336**
	0.2	1	2	6	9	16	47	**4360**	**4344**	**4329**
	0.1	1	1	4	7	12	23	**4353**	**4338**	**4322**
		0.1	0.2	0.3	0.4	0.5	0.6	0.7	0.8	0.9
						Ψ				

Table 6. Results of Non-linear Reverse Routing of the single step wave of duration 10 hours

	0.9	1	1	1	1	4	6	9	18	85
	0.8	1	1	1	4	5	9	17	75	**4772**
	0.7	1	1	4	5	8	16	67	**4856**	**4667**
	0.6	1	3	5	7	15	42	89	**4736**	**4630**
ϑ	0.5	3	4	7	13	30	55	**4830**	**4679**	**4601**
	0.4	3	5	7	12	34	70	**4743**	**4642**	**4575**
	0.3	1	4	6	9	18	89	**4690**	**4611**	**4553**
	0.2	1	2	5	7	12	30	**4653**	**4586**	**4534**
	0.1	1	1	3	6	9	16	84	**4563**	**4517**
		0.1	0.2	0.3	0.4	0.5	0.6	0.7	0.8	0.9
						Ψ				

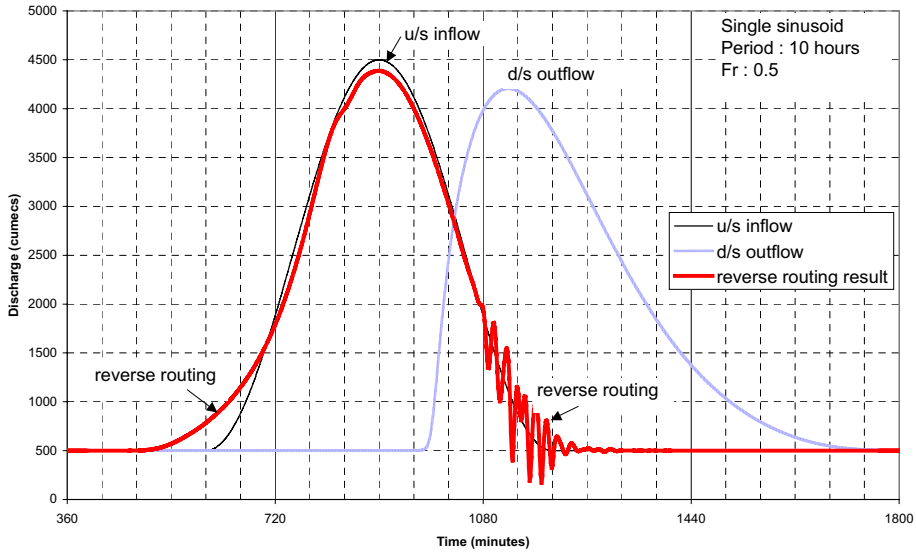

Fig. 7. *Reverse routing of a single cycle of period 10 hours*

peak. Some oscillations have begun to build up at the tail of the recession. However, for the flash flood, with a period of 1hour (Figs. 9 and 10), the high-frequency detail has been substantially attenuated and is not recovered in the reverse routing. The reverse routed hydrographs are smoother and broader than the original inflows. The peak of the reverse routed hydrograph is one-third of the original inflow peak. Similar results are obtained for the step functions (Fig. 11).

Figure 9 shows the periodogram for the upstream inflow, downstream outflow and best reverse routed inflow for the case of the single sinusoid of period (T) 1 hour. While the upstream inflow does contain contributions from all periods from 0.1 to 10 hours, there is a marked reduction in amplitude with reduction in period (higher frequency). The forward routing reduces the higher frequencies even more, giving a downstream outflow with little information, only noise, for periods below 20 minutes. The reverse routing fails to recover the shape of the original upstream inflow periodgram and actually contains more short period (high frequency) components than the original. This demonstrates the growth of high frequency noise in the reverse routing process.

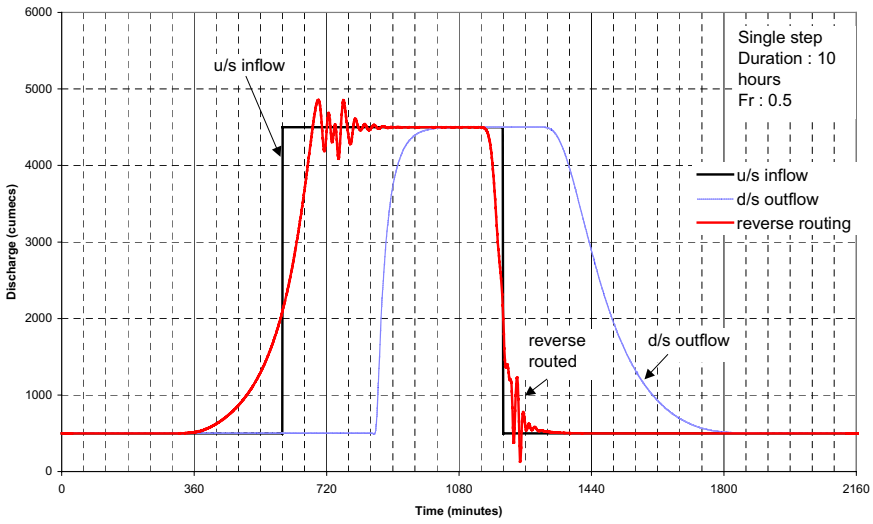

Fig. 8. *Reverse routing of a step of duration 10 hours*

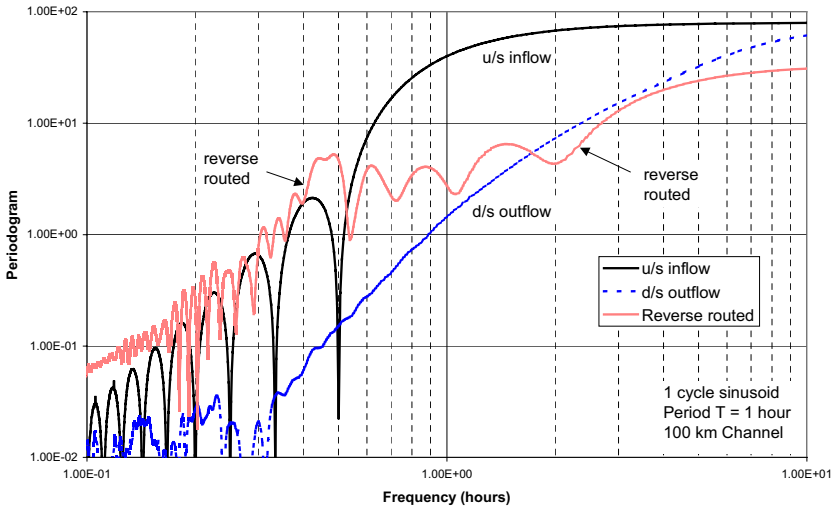

Fig. 9. *Build-up of high frequencies in reverse routing (for single sinusoid case with reriod T = 1 hour)*

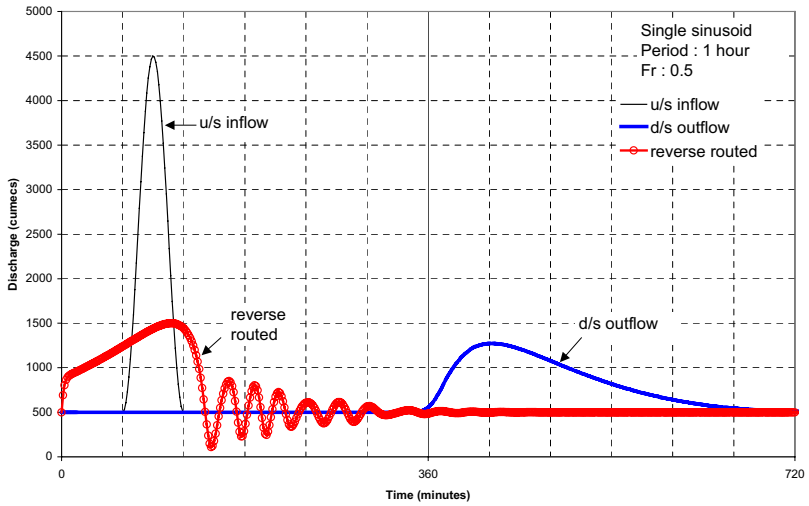

Fig. 10. *Reverse routing of a single cycle of period 1 hour*

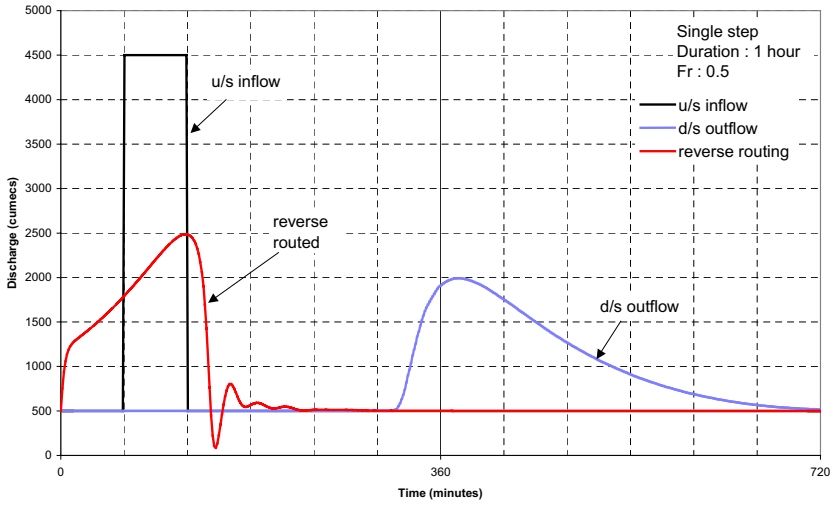

Fig. 11. *Reverse routing of a step of duration 1 hour*

Conclusions

The properties of a numerical procedure for reverse routing have been investigated. Despite the problem being mathematically ill-posed , reverse routing is shown to be possible for long channel lengths (> 100 km) in prismatic channels. It can give reasonably accurate results for long period waves, for which the general shape and peak flow are well recovered.

However, for short period waves (flash floods, in this case of period 1 hour), the reverse routing generates high frequency noise which ultimately limits the upstream reverse routing distance which can be achieved. The noise build-up appears to begin at the end of recessions and at discontinuities (e.g. in the case of the step) in the hydrograph. In addition, the reverse routing is unable to recover the high frequency components of the upstream inflow which have been attenuated strongly by the forward routing. The calculated reverse routed hydrographs are then very different from the original upstream inflows.

These results are influenced by the channel morphology and shape of the wave. Further work is needed to determine how these factors interact.

References

Bautista, E., Clemens, E.J. and Strelkoff, T., 1997. Comparison of Numerical Procedures for gate stroking. *J. Irrig. Drain. Eng.-ASCE*, **123**, 129–136.

Bodley, W.E. and Wylie, F.B., 1978. Control of transients in series of channels and gates. ***J.*** *Hydraul. Div.- ASCE*, **104** (HY10), 1395–1407.

Bruen, M. and Dooge, J.C.I., 1999. *Flash flood control using reverse routing*. Technical Report on TELFLOOD Project, Centre for Water Resources Research, University College Dublin. Ireland. 48pp.

Chatfield, C., 1975. *The analysis of time series: theory and practice.* Chapman & Hall, London, UK. 263pp

Clemens, A.J., (Ed.), 1998. Canal Automation. *J. Irrig. Drain. Eng.-ASCE*, **124**, Special Issue, 1–63.

Dooge, J.C.I. and Bruen, M., 2005. Problems in Reverse Routing. *Acta Geophysica Polonica,* **53,** 357–371.

Nachlik, E. and Witt, M., 1990. *Application of hydrodynamic models of flood wave propagation in the Upper Vistula river systems in flood protection of the basin*. Report No. CPBR 11.10.5.25. Technical University of Cracow. (in Polish).

Nachlik, E. and Witt, M., 1993. Hydraulic models of outflow control in Upper Vistula system. *Proc. Int. Conf. Hydroscience and Engineering*, Washington, USA.

Napiórkowski, J.J., 1992. Linear theory of open channel flow. In: *Advances in Theoretical Hydrology – A tribute to James Dooge*, J.P.O'Kane (Ed.), Elsevier, Amsterdam, The Netherlands. 254pp.

Preissman, A., 1961. *Propagation des intumescences dans les canaux et rivieres*. 1er Congres de l'Assoc. Francaise de Calcul, Grenoble, France. 433–442.

Saint-Venant, B. de, 1871. Théorie de Liquids non-permanent des eaux avec application aux cave des rivieres et à l'introduction des marées dans leur lit. (Theory of the unsteady movement of water with application to river floods and the introduction of tidal floods in their river beds.) *Acad. Sci. Comptes Rendus,* **73**, 148–154 and **33**, 237–249.

Szollogzi-Nagy, A., 1987. Input detection by the discrete linear cascade. *J. Hydrol*., **89**, 353–370.

Szymkiewicz, R., 1993. Solution of the inverse problem for the Saint Venant equations. *J. Hydrol.***, 147**, 105–120.

Szymkiewicz, R., 1996. Numerical stability of implicit four-points scheme applied to inverse linear flood routing. *J. Hydrol***., 176**, 13–23.